

An Implicit Rotor Speed Computation Algorithm for Squirrel Cage Induction Motor

C. Nagamani, M. A. Asha Rani, G. Saravana Ilango, Nikhilesh Prasanna Kumar

Dept. of Electrical and Electronics

National Institute of Technology, Tiruchirappalli, India

Abstract-- A novel method of sensor-less speed computation for squirrel cage induction motor is proposed. The algorithm enables computation of the rotor speed without the need for explicit computation of stator or rotor flux. The technique involves calculation of rotor currents from stator voltages and currents without the need for frame transformations, and computation of supply frequency without inverse trigonometry calculations or recursive procedures which lead to signal attenuation, noise and time delay in estimation. Further, the technique is quite versatile since the computed speed is accurate even under fluctuating loads or grid conditions such as fluctuating supply voltage and/or frequency, unbalanced voltage or presence of harmonics in supply voltage. The efficacy of the algorithm is verified using a laboratory machine with a generic digital signal processor. Though it is an open loop technique, the sensitivity to parameter variations is found to be insignificant and the accuracy is comparable to closed loop estimation techniques such as MRAS. Nearly zero steady state error and a worst case transient error less than 5% during load changes or during voltage and frequency fluctuations are observed.

Index Terms-- Squirrel cage induction motor, sensor-less speed computation, load changes, input fluctuations, unbalance.

I. INTRODUCTION

The motivation for reducing the cost and improving the robustness and reliability of the system in closed loop control of induction machines has increased the research focus on sensor-less speed computation techniques, which eliminate the need for any external sensors or interfacing [1].

Sensor-less speed computation schemes overcome the limitations of external sensor based systems by relying on secondary measurements to estimate or compute the rotor speed. Usually, measurements such as the stator and rotor voltages and currents as well as the phase differences between these quantities are used in computing or estimating the rotor speed. Various speed estimation methods have been reported in the literature. They can broadly be classified as: (i) model based methods and (ii) signal injection based methods. Signal injection involves the addition of a high frequency signal to the input voltage of the machine and then observing and quantifying how the injected signal is modified by the machine. Signal injection based methods perform well at zero-speed and exhibit low parameter sensitivity [2]. However, at higher speeds, signal injection suffers from the adverse effect of injected signal on the machine's performance.

On the other hand, model based methods are simpler in comparison to signal injection. These methods rely on the mathematical model of the induction machine to estimate or

compute the rotor speed based on stator and rotor voltages as well as currents. But, they suffer from parameter sensitivity as well as observability problems at low speed [3]. Further, the model based methods fall under two broad categories - open loop and closed loop. Voltage / Current Model based schemes usually fall under the open loop category while most MRAS as well as Adaptive Observer based techniques are of closed loop nature. In MRAS based methods, an error signal used to drive the adaptation mechanism is derived either from the current or flux in the rotor or stator [4]. These algorithms require an ideal integrator in the reference model. Based on the relationship between the stator and rotor currents with a constant flux, the rotor speed can be estimated. A few other closed loop schemes employ low-pass filters with either a fixed or a variable cut-off frequency [5], offset compensation along with pure integration [6] and phase locked loop with programmable low-pass filter [7]. Rotor speed is obtained through the phase comparison of actual and estimated rotor currents using a closed loop PI or hysteresis controller. The estimation of rotor current is based on air gap power vector [8] or a speed adaptive reduced order observer [9].

Open loop position estimation schemes employ either a voltage integrator for the flux estimation [10], or depend upon inverse trigonometric computations in real time [11], or recursive procedures [12]. Some of these schemes suffer from saturation in the integration stage or at various stages of the process. A sensorless position/speed computation algorithm for doubly fed induction machines [13] employed the measured stator voltage and stator and rotor currents to compute the resolved stator flux components. These were implicitly used to compute the rotor position. However, the rotor speed computation involved differentiation of rotor position. Rotor flux position estimation involved voltage integration [16], or adding the slip angle to the rotor angle [17]. Inverse trigonometric computations and integration of torque angle and hence delay in estimation are observed in [18].

This paper proposes a method for direct computation of rotor speed algorithm without estimation of flux or rotor position. Rotor currents and supply frequency are computed from the measured stator voltages and currents in a straight forward manner. These are further used to compute the rotor speed.

II. IMPLICIT ROTOR SPEED COMPUTATION ALGORITHM

The proposed implicit rotor speed computation algorithm (IRSCA) for squirrel cage induction motors is an extension of the technique described in [13]. The rotor currents are computed from stator voltages and currents without the need

for frame transformations, while computation of supply frequency is done without inverse trigonometry calculations or recursive procedures which lead to signal attenuation, noise and time delay in estimation. The method does not require the estimation of any quantity and hence is immune to the drawbacks associated with estimators. By computing the resolved flux components in terms of analytical equivalents, complex arithmetic such as inverse trigonometry and recursive algorithms are eliminated. Thus it is an implicit computation algorithm based merely on the machine model.

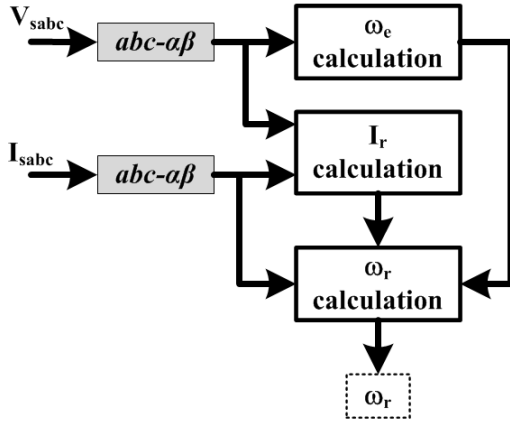


Fig. 1. Block Diagram of IRSCA.

There are three major steps involved in the proposed computation algorithm – the calculation of supply frequency, the computation of rotor currents and finally the calculation of the rotor speed. As seen from the basic block diagram (Fig. 1), the measured three phase stator voltages and currents are first transformed to the stationary α - β reference frame. The stator voltage is then used to calculate the supply frequency, ω_e which is subsequently used in the calculation of the rotor speed. Further the stator voltages ($V_{s\alpha}$, $V_{s\beta}$), along with the stator currents ($i_{s\alpha}$, $i_{s\beta}$), are used for the computation of rotor currents ($i_{r\alpha}$, $i_{r\beta}$). The rotor currents are directly computed in the stator reference frame, negating the need for any further reference frame transformation operations.

Finally, the stator and rotor currents, along with the supply frequency computed earlier, are used to compute the rotor speed of the machine. A key feature of this algorithm is the fact that the rotor currents in the stationary reference frame are calculated in a straightforward manner without the estimation of stator flux or stator magnetizing current. The procedure is based on substitutions for the stator flux components in terms of the measured stator voltage and currents. These substitutions eliminate the need for flux estimation. The spatial distribution of the relevant space vectors are shown in (Fig. 2).

The stator flux in the stationary reference frame can be expressed as,

$$\varphi_{s\alpha} = L_s i_{s\alpha} + L_m i_{r\alpha} \quad (1)$$

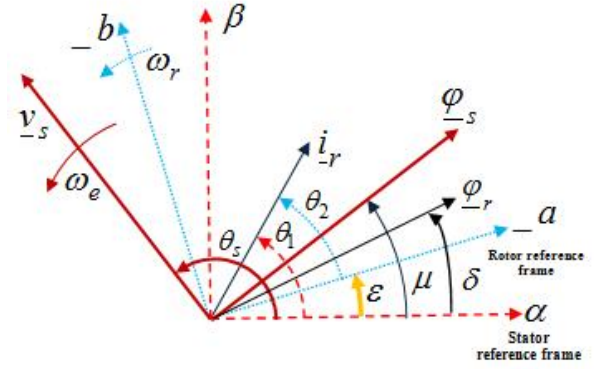


Fig. 2. Spatial Distribution of Space Vectors

$$\varphi_{s\beta} = L_s i_{s\beta} + L_m i_{r\beta} \quad (2)$$

Rearranging (1) and (2), the rotor currents can be expressed as

$$i_{r\alpha} = \frac{(\varphi_{s\alpha} - L_s i_{s\alpha})}{L_m} \quad (3)$$

$$i_{r\beta} = \frac{(\varphi_{s\beta} - L_s i_{s\beta})}{L_m} \quad (4)$$

The expressions for rotor current in (3) and (4) contain the components of the stator flux. These components can be expressed in terms of other known variables, based on the induction machine model. From the machine model, the stator voltage components in the stationary reference frame can be represented as,

$$v_{s\alpha} = R_s i_{s\alpha} + \frac{d}{dt} \varphi_{s\alpha} \quad (5)$$

$$v_{s\beta} = R_s i_{s\beta} + \frac{d}{dt} \varphi_{s\beta} \quad (6)$$

Since, the total stator magnetizing flux is oriented along the d -axis in the synchronous reference frame, the components of stator flux in stationary reference frame can be expressed as

$$\varphi_{s\alpha} = |\varphi_s| \cos(\mu) \quad (7)$$

$$\varphi_{s\beta} = |\varphi_s| \sin(\mu) \quad (8)$$

where μ is the angle between synchronous and stator reference frames. The stator fluxes as well as the angle μ are time varying quantities. Therefore, differentiating the flux components (7) and (8) with respect to time gives,

$$\frac{d}{dt} \varphi_{s\alpha} = \left[\frac{d}{dt} |\varphi_s| \right] \cos(\mu) - |\varphi_s| \sin(\mu) \frac{d\mu}{dt} = \left[\frac{d}{dt} |\varphi_s| \right] \cos(\mu) - \varphi_{s\beta} (\omega_e) \quad (9)$$

$$\equiv -\varphi_{s\beta} \omega_e$$

$$\frac{d}{dt} \varphi_{s\beta} = \left[\frac{d}{dt} |\varphi_s| \right] \sin(\mu) + |\varphi_s| \cos(\mu) \frac{d\mu}{dt} = \left[\frac{d}{dt} |\varphi_s| \right] \sin(\mu) + \varphi_{s\alpha} (\omega_e) \quad (10)$$

$$\equiv \varphi_{s\alpha} \omega_e$$

where $\frac{d}{dt}(\mu) = \omega_e$. The rate of change of the magnitude of stator flux with time can be considered to be negligibly small under normal grid conditions. This is owing to the fact that the

prevailing grid codes limit the permissible fluctuation in voltage and frequency to a very small margin. This margin is sufficiently small for the time derivative of stator flux magnitude to be negligibly small. Thus (5) and (6) can be simplified to (11) and (12) as

$$v_{s\alpha} = R_s i_{s\alpha} - \omega_e L_s i_{s\beta} - \omega_e L_m i_{r\beta} \quad (11)$$

$$v_{s\beta} = R_s i_{s\beta} + \omega_e L_s i_{s\alpha} + \omega_e L_m i_{r\alpha} \quad (12)$$

By rearranging the terms in (11) and (12), the rotor current can be implicitly computed in terms of known measured quantities, namely supply frequency, stator voltage and current. Thus the rotor current can be computed in the stationary reference frame. This eliminates the need for further reference frame transformations in order to compute the rotor speed.

$$i_{r\alpha} = \frac{v_{s\beta} - R_s i_{s\beta} - \omega_e L_s i_{s\alpha}}{\omega_e L_m} \quad (13)$$

$$i_{r\beta} = \frac{R_s i_{s\alpha} - v_{s\alpha} - \omega_e L_s i_{s\beta}}{\omega_e L_m} \quad (14)$$

The equations (13) and (14) are the principal feature of the algorithm which renders it significantly simple and as accurate as the machine model. As opposed to (3) and (4), (13) and (14) render the computation of rotor current free of the stator flux terms and thus making the computation of $i_{r\alpha}$ and $i_{r\beta}$ implicit. With the rotor currents implicitly computed, the rotor speed can now be calculated easily. Using the machine equations for the rotor in the stationary reference frame, the rotor voltage components can be expressed as,

$$v_{r\alpha} = R_r i_{r\alpha} + \frac{d}{dt} \phi_{r\alpha} + \omega_r \phi_{r\beta} \quad (15)$$

$$v_{r\beta} = R_r i_{r\beta} + \frac{d}{dt} \phi_{r\beta} - \omega_r \phi_{r\alpha} \quad (16)$$

For a squirrel cage induction machine, $V_{r\alpha}$ and $V_{r\beta}$ are equal to zero since the rotor windings are short circuited. Therefore, the rotor speed can now be computed by substituting the derivative of rotor flux in (15) in a similar fashion as in (11) and (12).

Thus speed can be computed from $V_{r\alpha}$ as

$$v_{r\alpha} = R_r i_{r\alpha} - \phi_{r\beta} (\omega_e) + \omega_r \phi_{r\beta} \quad (17)$$

Further (17) can be rearranged to compute speed by substituting $V_{r\alpha} = 0$ (short circuited rotor) as shown below.

$$\omega_{r(\text{computed})} = \omega_e - \frac{R_r i_{r\alpha}}{L_r i_{r\beta} + L_m i_{s\beta}} \quad (18)$$

The computed rotor speed requires only the values of stator and rotor currents in the stationary reference frame, which are available from (13) and (14). Thus there is no need for any estimation of flux or magnetizing current. Further, the computation scheme is free from integration. As seen from (13) to (18), the IRSCA only uses basic mathematic operations on the measured instantaneous stator voltages and currents.

III. VALIDATION OF THE ALGORITHM

The efficacy of the sensorless speed computation algorithm is tested by means of extensive MATLAB/Simulink based

computer simulations. The adaptability of the algorithm to rapid changes in operating conditions is a crucial factor that affects the performance of the motor drive system. The test machine is subjected to a variety of fluctuations in input supply as well as load conditions so as to induce speed variations. During the course of the simulations, the load on the machine is varied with time as specified in Table I. Also, supply voltage and frequency fluctuations are considered as detailed in Table II. Unbalance and harmonics in the power supply are the common power quality issues faced by power systems. This can cause ripple in the rotor speed and can result in sustained errors in the speed computation process thus affecting the accuracy. Hence, the effect of unbalance and harmonics on the algorithm is also investigated.

Table I. Variations in Load Torque

Time (s)	Load Torque
0 < t < 1	0 Nm
1 < t < 3	6 Nm
3 < t < 5	0 Nm
5 < t < 6	3 Nm
6 < t < 7	6 Nm
7 < t < 8	10 Nm
8 < t < 10	6 Nm

Table II: Variations in Voltage and Frequency

Event	Time (s)
Voltage Increase (10%)	2.0
Voltage Decrease (10%)	2.8
Frequency Increase (5%)	3.0
Frequency Decrease (5%)	3.8
Voltage and Frequency Increase	4.0
Voltage and Frequency Decrease	4.8
Voltage Increase and Frequency Decrease	5.0
Voltage Decrease and Frequency Increase	6.0

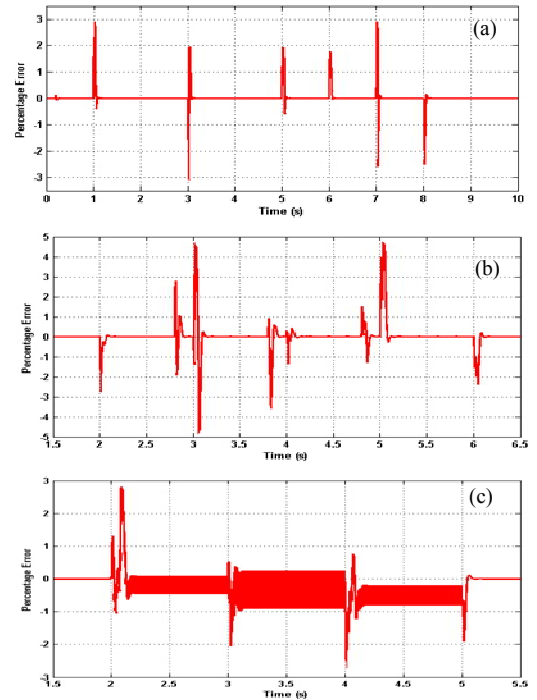


Fig. 3. Error between Actual and Computed Speed during (a) Load Changes (b) Voltage and Frequency fluctuations (c) Unbalance and Harmonics.

The variation of actual and computed rotor speed during load changes, voltage and frequency fluctuations and with unbalance and harmonics are illustrated in (Fig.3 (a), (b) and (c)) respectively. The comparison of the steady state error of the IRSCA with that of an MRAS based scheme [14] is illustrated in Table III. Despite being an open loop algorithm, the IRSCA did not exhibit any steady state error during load changes as well as voltage and frequency fluctuations. The presence of harmonics or unbalance leads to slight steady state errors. The steady state error is around 0.85 to 0.95% only, which is comparable to that of closed loop MRAS based schemes. Further, the transient errors of the IRSCA are compared with an MRAS based scheme in Table IV. The transient errors are only marginally higher than that of a MRAS based technique. The errors range from 1.2% to a worst case error of 5%. As the algorithm is open loop and directly based on the measured values of voltage and current, any transient present in the input signals will result in a transient in the output as well. Further, changes in frequency can produce a transient in the computed supply frequency as well. This phenomenon can be observed with the transient errors during voltage and frequency changes. However, the error during a simultaneous voltage and frequency increase or decrease is significantly lesser than the error during a voltage change together with an opposing frequency change.

Table III. Error during Steady State Operation

Operating Condition	IRSCA	MRAS
Load changes (No load – full load)	0 %	0 %
Voltage changes (10%)	0 %	0 %
Frequency changes (5%)	0 %	0 %
Voltage and frequency changes (10%, 5%)	0 %	0 %
Harmonics (10%)	0.85 %	0.55 %
Harmonics and unbalance (10%)	0.95 %	0.45 %

Table IV. Error during Transient State

Operating Condition	IRSCA	MRAS
Load increase	3.0 %	2.0 %
Load decrease	3.0 %	2.0 %
Voltage increase	2.2 %	1.2 %
Voltage decrease	2.2 %	1.2 %
Frequency increase	5.0 %	2.0 %
Frequency decrease	3.2 %	2.2 %
Voltage and frequency increase	1.2 %	3.0 %
Voltage and frequency decrease	1.5 %	3.0 %
Voltage increase and frequency decrease	5.0 %	1.5 %
Voltage decrease and frequency increase	2.2 %	2.0 %
Harmonics	3.0 %	1.0 %
Unbalance and harmonics	3.0 %	1.0 %

IV. HARDWARE IMPLEMENTATION

A novel generic motor control hardware system based on the C2000 family of Digital Signal Controllers from Texas Instruments was developed for the implementation and testing of the proposed IRSCA. The hardware system, based on the C2000 LaunchPad featuring the TMS320F28027F DSC, has extensive capabilities, including a 13-channel ADC, 8 PWM outputs, (Texas Instruments, 2012) an 8-channel DAC as well as digital input/output as well as safety features such as emergency trip. A block diagram of the hardware setup is shown in (Fig.4). Using the hardware setup (Fig.5), the

performance of the IRSCA was evaluated on the laboratory 1 hp induction machine.

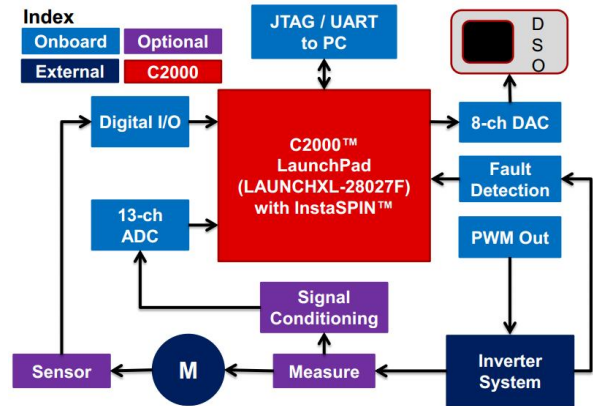


Fig. 4. Schematic of hardware setup.



Fig. 5. Photograph of the hardware setup.

The three-phase supply to the system is provided through an autotransformer. The voltages and currents were measured using closed loop hall-effect based voltage and current transducers, coupled with an appropriate signal conditioning circuitry. The accuracy of the speed computation algorithm was tested by comparing the output of the algorithm with the speed measured using a contactless optical speed sensor. The transient and steady state performance during a sudden change in load from no load to full load was observed. The load change was effected by loading the mechanically coupled DC generator with a large resistive load.

V. RESULTS AND DISCUSSION

The performance during the starting up of the machine was also observed (Fig.6 (a)). It is notable that the algorithm starts tracking the rotor speed almost immediately from 228 rpm onwards to 1460 rpm. Subsequent to the start-up, a load change operation is performed as shown in (Fig.6 (b)) from no load to full load and back to no load (speed change from 1480 rpm to 1360 rpm and back to 1480 rpm) to observe the transient and steady state performance. Further, the performance of IRSCA was tested for speed variations in the sub synchronous (1471 rpm to 1375 rpm and back to 1471 rpm) and super synchronous regions (1420 rpm → 1477 rpm → 1512 rpm) (Fig.6(c)) respectively. It is notable that the hardware results correlate with the computer simulation

studies, showing negligible error during steady state. During load change and speed variations, the transient error was found to be within 2.5 to 3.5 %, as predicted by the computer simulations. The IRSCA enables accurate tracking of speed

even during the starting of the induction machine and also during transition from sub synchronous to super synchronous speeds. The behaviour during load change is also successfully tracked by the IRSCA with a transient error of about 3%.

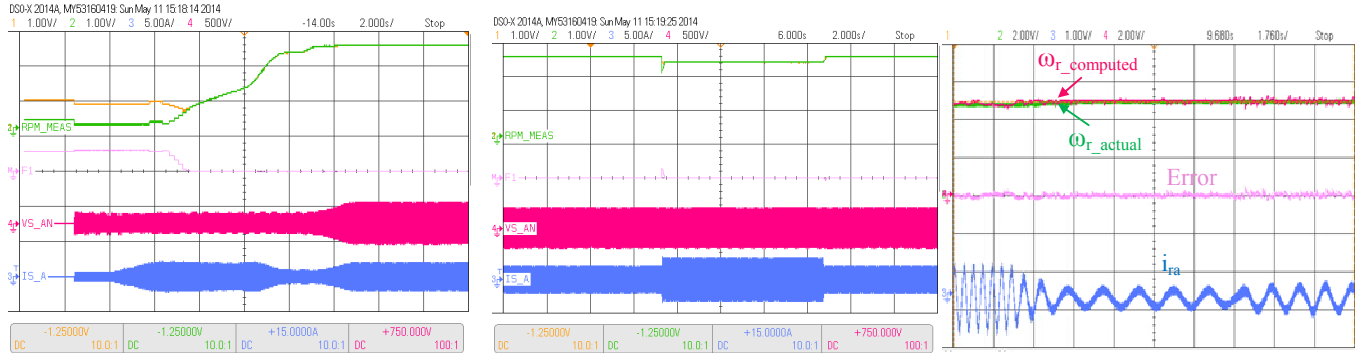


Fig.6. (a) & (b) Stator Voltage, Stator Current, Actual and Computed Rotor Speed and Error in speed computation during starting up of motor and no-load to full load change respectively and (c) Rotor Current, Actual and Computed Rotor Speed and Error in speed computation during speed variations.

VI. CONCLUSIONS

A new, simplified and implicit rotor speed computation algorithm for squirrel cage induction machines has been proposed in this paper. The scheme is straightforward and computationally very simple enabling it to be easily used for real-time speed control of an induction machine. The algorithm requires only basic mathematical operations and there is no requirement of inverse trigonometry or other intensive computations and does not involve the estimation of any quantity. The simplicity of the IRSCA enables it to be easily deployed on low cost fixed point digital signal processors or microcontrollers. The IRSCA performs quite well under all conditions with no steady state error, except under the presence of voltage unbalance or harmonics. The transient error is less than 2-3% under most conditions with a worst case error of just 5% under parameter variations. The overall efficacy of the open loop IRSCA is comparable to that of a closed loop MRAS based estimation scheme.

VII. APPENDIX

TABLE V - Parameters of Squirrel Cage Induction Machine

Parameter	Symbol	Actual value in SI units
Stator resistance	R_s	4.12 Ω
Rotor Resistance	R_r	5.26 Ω
Leakage inductance of stator	L_{ls}	28 mH
Leakage inductance of rotor	L_{lr}	28mH
Mutual inductance	L_m	27 mH
Moment of Inertia	J	0.14 $\text{kg}\cdot\text{m}^2$
Friction coefficient	B	0.03 $\text{kg}\cdot\text{m}^2/\text{s}$

VIII. REFERENCES

- [1] C. Canudas De Wit, A. Youssef, J. P. Barbot, P. Martin and F. Malrait, "Observability conditions of induction motors at low frequencies", in *Proc. of 39th IEEE Decision and Control Conf.*, pp. 2044-2049, 2000.
- [2] Jung-Ik Ha and Seung-Ki Sul, "Sensorless field-orientation control of an induction machine by high-frequency signal injection", *IEEE Trans. Ind. Appl.*, vol. 35, pp. 45-51, Feb. 1999.
- [3] Cao-Minh Ta, T. Uchida and Y. Hori, "MRAS based speed sensorless control for induction motor drives using instantaneous reactive power", in *Proc. of IEEE-IECON Conf.*, pp. 1417-1422, 2001.
- [4] H.M.Kojabadi, "Simulation and experimental studies of model reference adaptive system for sensorless induction motor drive", *Simulation Modelling Practice and Theory*, vol. 13, pp. 451-464, 2005.
- [5] Sheng Yang and Venkataramana Ajjarapu, "A Speed-Adaptive Reduced-Order Observer for Sensorless Vector Control of Doubly Fed Induction Generator-Based Variable-Speed Wind Turbines", *IEEE Trans. Energy Conv.*, vol. 25, pp. 891-900, 2010.
- [6] Mihai Comanescu and Longya Xu, "An improved flux observer based on PLL frequency estimator for sensorless vector control of induction motors", *IEEE Trans. Indus. Elec.*, vol. 53, pp. 50-56, 2006.
- [7] Bakari Mwinyiwiwa, Yongzheng Zhang, Baikeshen and Boon-Teck Ooi, "Rotor Position Phase-Locked Loop for Decoupled P-Q Control of DFIG for Wind Power Generation", *IEEE Trans. Energy Conv.*, vol. 24, pp. 758-765, 2009.
- [8] Fang-Zheng Peng and T. Fukao, "Robust speed identification for speed sensorless vector control of induction motors", *IEEE Trans. Ind. Appl.*, vol. 30, pp. 1234-1240, 1994.
- [9] M. Cirrincione, M. Pucci, G. Cirrincione and G. A. Capolino, "A new adaptive integration methodology for estimating flux in induction machine drives", *IEEE Trans. Power Elec.*, vol. 19, pp. 25-34, 2004.
- [10] L. Morel, H. Godfroid, A. Mirzaian and J. M. Kauffmann, "Double-fed induction machine: Converter optimization and field oriented control without position sensor", in *Proc. of IEE Electrical Power Appl. Conf.*, vol. 145, pp. 360-368, 1998.
- [11] Mehdi T. Abolhassani, Prasad Enjeti and Hamid Toliyat, "Integrated doubly fed electric alternator/active filter (IDEA), a viable power quality solution, for wind energy conversion systems", *IEEE Trans. Energy Conv.*, vol. 23, pp. 642-650, 2008.
- [12] Amit Kumar Jain and V. T. Ranganathan, "Wound Rotor Induction Generator with Sensorless Control and Integrated Active Filter for Feeding Nonlinear Loads in a Stand-Alone Grid", *IEEE Trans. Ind. Elec.*, vol. 55, pp. 218-228, 2008.
- [13] A. Karthikeyan, C. Nagamani and Aritra Basu Ray Chaudhury, "An Implicit Sensorless Position/Speed Estimator for the speed control of a Doubly Fed Induction Motor", in *Proc. of IEEE PES Innov. Smart Grid Tech. Conf. India*, pp. 120-125, 2011.
- [14] Suman Maiti, Chandan Chakraborty, Yoichi Hori and Minh C. Ta, "Model reference adaptive controller-based rotor resistance and speed estimation techniques for vector controlled induction motor drive utilizing reactive power", *IEEE Trans. Ind. Elec.*, vol. 55, pp. 594-601, 2008.
- [15] Texas Instruments, "LAUNCHXL-F28027 C2000 Piccolo LaunchPad Experimenter Kit Users Guide", 2012.
- [16] G. Poddar and V. T. Ranganathan, "Sensorless Double-Inverter-Fed Wound-Rotor Induction-Machine Drive", *IEEE Trans. Indus. Elec.*, vol. 53, pp. 86-95, 2006.
- [17] Scott Wade, Matthew W. Dunnigan and Barry W. Williams, "Modeling and Simulation of Induction Machine Vector Control with Rotor Resistance Identification", *IEEE Trans. Power Elec.*, vol. 12, pp. 495-505, 1997.

- [18] Longya Xu and Wei Cheng, "Torque and Reactive Power Control of a Doubly Fed Induction Machine by Position Sensorless Scheme", *IEEE Trans. Ind. Appl.*, vol. 31, pp. 636-642, 1995.